Academic Journal of Science and Technology
ISSN: 2771-3032 | Vol. 5, No. 3, 2023

Analysis and Experimental Study on Location Exploration of Relief Well

Xiaoyu Zhu

School of Electrical Information Engineering, Northeast Petroleum University, Daqing 163319, China

Abstract: As oil and gas extraction continues to expand and deepen, the importance of relief wells becomes increasingly evident. The positioning and detection technology of relief wells is a critical technology that plays a significant role in ensuring the safety and success of relief well construction. This article focuses on the positioning and detection technology of relief wells, analyzing existing technologies and identifying issues such as difficulties in trajectory control and susceptibility to magnetic field interference, leading to low positioning accuracy and ineffective relief wells. To address these problems, simulation experiments were conducted using coils and probes on an experimental platform to replicate the positioning and detection measurements of relief wells, followed by comprehensive analysis of the experimental data.

Keywords: Relief well, Electromagnetic, Trajectory Control, Laboratory experiment.

1. Introduction

As China's shallow oil and gas resources are becoming increasingly depleted and the country's dependence on foreign crude oil remains high, ensuring energy security is an urgent task. Oil and gas production is a highly complex, risky, and unpredictable task. In the event of a high-pressure blowout, the losses can be enormous. Therefore, it is essential to improve emergency response capabilities to contain major safety accidents. When conventional emergency response measures fail, relief wells become the last resort for pressure relief operations. However, in practice, the construction of relief wells faces certain challenges, such as significant cumulative errors in downhole measurements and the high precision required for trajectory control. Currently, active magnetic measurement technology is widely used for positioning accident wells to guide the connection of relief wells to the accident well. However, there is a risk of failure associated with the direct field application of this technology, and as such, simulation experiments are needed to provide data support for algorithm improvements and field applications.

2. Distance Calculation Method

The relief well and accident well connection detection system, illustrated in Figure 1, comprises a ground box, surface electrode, probe, downhole linear electrode, and surface computing software system. The current propagation in the relief well detection system is analogous to the current propagation between multi-layer columnar bodies with different media conductivity. However, due to the high conductivity of the accident well casing, the current flowing between wells will mostly accumulate on the accident well casing, resulting in a low-frequency alternating current that travels up and down the casing. As per Ampere's law, this alternating current generates a low-frequency alternating magnetic field.

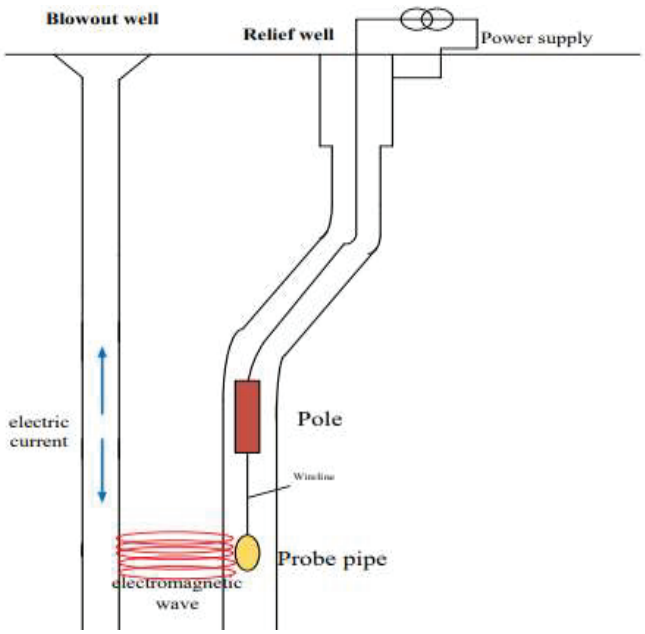

Figure 1. Schematic diagram of communication detection system between relief well and accident well.

The process of current propagating through the formation and converging at the casing of the accident well, resulting in the production of an alternating magnetic field, conforms with the Maxwell equations. By deriving the Maxwell equation group, the Helmholtz equation under the condition of a time-harmonic field can be obtained:

$$\begin{aligned}\nabla^2\vec{E}+\omega^2\mu\varepsilon\vec{E}=0\\ \nabla^2\vec{H}+\omega^2\mu\varepsilon\vec{H}=0\end{aligned} \tag{1}$$

In this context, $\vec{H}$ denotes the magnetic field intensity generated by the external excitation source, measured in Tesla (T); $\vec{E}$ represents the electric field strength produced by the external excitation source, measured in volts per meter (V/m); μ refers to the permeability, measured in henries per meter (H/m); and ε denotes the permittivity, measured in farads per meter (F/m).

In the region where the current element is present, the potential satisfies the Poisson's equation:

$$\nabla^2 U=\frac{\rho}{\varepsilon} \tag{2}$$

In a region that is both source-free and non-boundary, the electric potential satisfies the Laplace's equation:

$$\nabla^2 U=0 \tag{3}$$

In equations (2) and (3), ρ represents the charge density of the electrical excitation source in units of C/m³. U represents the potential generated by the current element in units of V.

The Poisson equation can be solved using Green's function, while Laplace's equation can be solved using the separation of variables method, together with the boundary conditions. By combining these methods and considering the boundary conditions, an equation can be obtained for the interface where $\rho=R_i$:

$$\begin{cases}U_i\,|_{\rho=R_i}=U_{i+1}\,|_{\rho=R_{i+1}}\\ \sigma_i\dfrac{\partial U_i}{\partial\rho}|_{\rho=R_i}=\sigma_{i+1}\dfrac{\partial U_{i+1}}{\partial\rho}|_{\rho=R_{i+1}}\end{cases} \tag{4}$$

Where, U_i denotes the electric potential of layer i and σ_i denotes the electrical conductivity of layer i.

Combining with Figure 2, we can derive an expression for the current $I(z)$ that converges on the casing of the accident well:

$$I(\mathrm{z})=\frac{r_e^{\,2}I_0}{2\pi}\int_0^{\infty}\frac{K_0(\lambda R)\sin\lambda\,\mathrm{z}}{r_c[I_1(\lambda\,\mathrm{r}_c)\mathrm{K}_0(\lambda\,\mathrm{r}_c)+\dfrac{\sigma_e}{\sigma_c}I_0(\lambda\,\mathrm{r}_c)\mathrm{K}_1(\lambda\,\mathrm{r}_c)]}d\lambda \tag{5}$$

In the above equation, r represents the distance between the two wells in meters, r_c is the casing radius of the accident well in meters, and r_e is the equivalent radius of the accident well after it has been transformed into a formation medium with the same impedance in meters. The relationship between r_c and r_e can be approximated as follows:

$$r_e=\sqrt{\frac{2\sigma_c}{\sigma_e}r_c d_c} \tag{6}$$

Here, σ_c and σ_e represent the conductivity of the casing and formation in S/m, respectively. d_c is the casing wall thickness of the accident well in meters. $I_1(\lambda\,\mathrm{r}_c)$ is the zero-order Bessel function of the first kind, while $\mathrm{K}_0(\lambda\,\mathrm{r}_c)$ is the zero-order Bessel function of the second kind. $\mathrm{K}_1(\lambda\,\mathrm{r}_c)$ is the first-order Bessel deformation function of the second kind. Finally, the variable R denotes the distance between the electrode and the casing, measured in meters.

As the casing is infinitely long, according to the Biot-Savart law, the magnetic field intensity on the casing is given by:

$$H(z)=\frac{I(z)}{2\pi r} \tag{7}$$

The variable "r" represents the distance between the detection tool and the casing of the accident well.

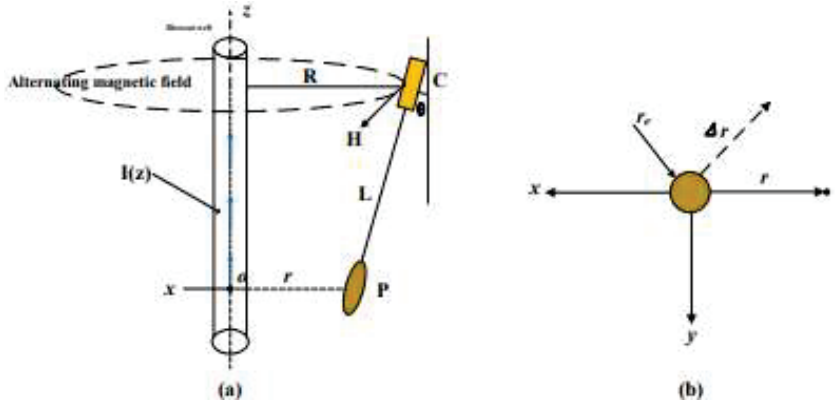

Figure 2. Geometric diagram of detection system

3. Experiment

3.1. Experimental apparatus

In this outdoor experiment, coils and probes are utilized to simulate the measurement of the relative position and distance between the relief well and the target well during drilling. The experimental platform, depicted in Figure 3, is designed with four wires forming a rectangular closed loop. P denotes the location of the probe, while the sensor is positioned on the central axis of the wire. The length of the straight wire in the loop, situated closer to the probe, is designated as L.

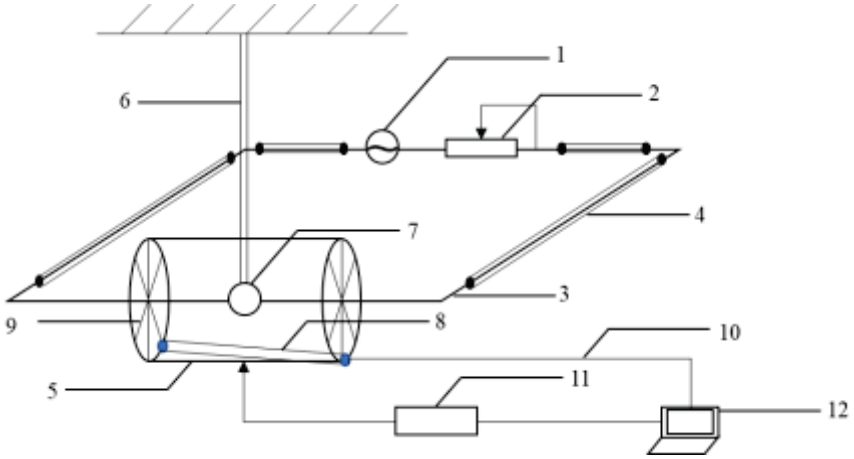

Figure 3. Schematic diagram of experimental setup.

1. Introduction to Experimental Setup.

The experimental setup is composed of an excitation system, detection system, control system, calibration system, and processing system. The schematic diagram of the setup depicts the various components, where numbers 1-12 correspond to: 1 excitation power supply, 2 variable resistors, 3 straight wires, 4 steel wire mesh, 5 platform, 6 cantilever, 7 turntable, 8 probe, 9 graduated dial, 10 cables, 11 hydraulic press, and 12 processing equipment (PC).

(1) Excitation System

The excitation system is designed to simulate the convergence of excitation current in the accident well column. It consists of an excitation power supply, variable resistors, straight wires, and steel wire mesh. The excitation power supply is capable of emitting AC current with a frequency range of 0.1-0.5 Hz and a current range of 0.1-10 A, which can display parameters such as the current magnitude and frequency in the circuit, effectively simulating the electrode and ground power source parts in real-world engineering scenarios. The variable resistor is used to adjust the secondary current and ensure that it doesn't overload. The straight wire is used to form a rectangular current loop, with one wire passing through the graduated dial of the platform to simulate the converging current in the accident well. The remaining three wires are wrapped in steel wire mesh to prevent the magnetic fields generated from interfering with the detection system of the relief well, which is situated away from the platform.

(2) Detection System

The detection system is used to simulate the signal of the changing magnetic field in the wellbore column of an accident well which is collected by the probe in the relief well and transmitted to the signal processing system. The relief well detection system includes a probe and a cable. The three-axis magnetic flux-gate sensors inside the probe collect the signal of the changing magnetic field in the wellbore column of the accident well, and the three-axis acceleration sensors collect the gravity acceleration value of the probe itself, which is transmitted to the processing system through the cable.

(3) Control System and Calibration System

During the experiment, the hydraulic control system is responsible for maintaining the relative position of the two wells, which consists of the frame, cantilever, hydraulic rotary table, and hydraulic press. The hydraulic press drives hydraulic oil to the hydraulic rotary table under the cantilever, which rotates the frame space and clamps the exploration pipe with hydraulic oil, simulating changes in the coordinates of the accident well and exploration pipe along a straight guide line.

Furthermore, the geometric calibration system consists of a dial gauge that accurately reflects the geometric position relationship of the simulated well. The hydraulic system controls the coordinates of the simulated accident well and exploration pipe in the straight guide line, which are then transmitted to the processing equipment. Overall, these processes work together to ensure a precise and accurate simulation of the experiment.

(4) Processing System

The processing system refers to a particular software application that runs on a PC located on the ground. Its main purpose is to utilize the Active Magnetic Measurement algorithm to compute the measurement position relationship of the simulated well. To simulate the error of the Active Magnetic Measurement in the experiment, the system compares the results obtained from the algorithm with geometric calibration values.

The system includes processing equipment 12, which carries out coordinate calculations to calculate the geometric position relationship of the simulated well. Then, using the Active Magnetic Measurement algorithm, the system calculates the measurement position relationship of the simulated well. Finally, the two sets of results are compared to evaluate the Active Magnetic Measurement's error accurately.

To summarize, the processing system utilizes the Active Magnetic Measurement algorithm and performs coordinate calculations to simulate errors occurring in Active Magnetic Measurements. It achieves this by comparing the geometric

position relationship of the simulated well and the measurement position relationship obtained from the algorithm.

3.2. Measurement methods

The dial gauge on the platform is illustrated in Figure 4, displaying the distance from the center (r) and the angle (θ) with reference to the vertical direction as the primary parameters. For ensuring the device's similarity to the actual working conditions, the other three straight leads in the circuit are shielded with wire mesh, effectively isolating the magnetic field. The replacement of the infinite-length relief well in Active Magnetic Measurement by a finite-length straight lead leads to the following derivation process:

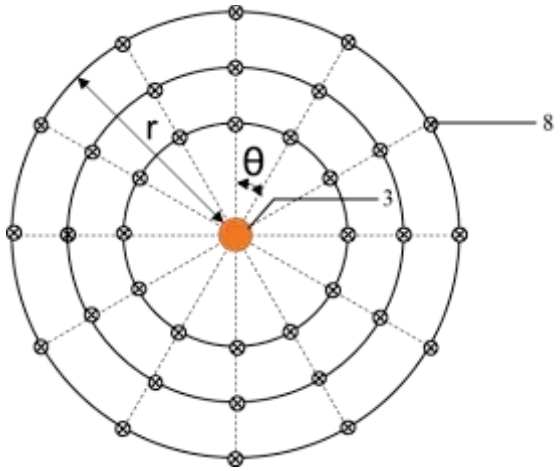

Figure 4. Schematic diagram of a graduated dial

According to the Biot-Savart Law, the magnetic field strength produced by a straight conductor with a length of L and carrying a current of I at a point r away is given by $B = \frac{\mu_0 I}{4\pi r}(\cos\theta_1 - \cos\theta_2)$, where θ_1 and θ_2 are the vectors that represent the distance between the two ends of the conductor and the magnetic flux gate sensor, respectively. Substituting the relevant data into equation (3-1), we obtain the produced magnetic field strength as follows:

$$B = \frac{\mu_0 I}{2\pi r}\frac{1}{\sqrt{(\frac{r}{L})^2 + 1}} \tag{8}$$

Under identical conditions, an infinite-length relief well casing produces a magnetic field strength of $B = \frac{\mu_0 I}{2\pi r}$. Therefore, a finite-length straight conductor of length 10m can be used to replace the infinite-length relief well casing in Active Magnetic Measurement when $r << L$. At this point, the edge of the dial gauge is 1m from the center and can be considered as an approximation of an infinite-length relief well. The value of r on the dial gauge is the geometric calibration distance, and θ is the geometric calibration direction.

3.3. Experimental procedure

During the experiment, a clockwise flow of control loop current was utilized, where the preset current value was 10A. The variable r represented the distance between the probe and the first straight conductor. The objective of the experiment was to observe and analyze the magnetic field strength effect created by flowing conductor at varied distances between the probe and the conductor. With the ability to simulate different parameters such as fluctuations in current, distance, and direction, the experiment sought to provide model parameters and practical data that would help advance the measurement algorithm and improve the control of the relief well trajectory.

(1) The hydraulic press system controls the relative position of the two wells in the hydraulic system;

(2) The power excitation system determines the excitation current value;

(3) The relief well detection system's probe records the alternating magnetic field signal;

(4) The processing system executes the Active Magnetic Measurement algorithm to determine the measurement position relationship of the simulated well;

(5) The acquired results are benchmarked against the geometric calibration system to calculate the Active Magnetic Measurement error;

(6) The process repeats steps (1) to (5) while changing the current, distance, and direction;

(7) The experiment is concluded, and the data is processed.

During the experiment, various scenarios of aggregated current under different formation parameters can be simulated by adjusting the current amplitude and frequency of the excitation current generated by the power source and repeating steps (2) to (5). This enables researchers to investigate the relationship between Active Magnetic Measurement (AMM) signal and error variation caused by changes in formation current.

To simulate different well spacing, the distance between the straight conductor and the probe (represented as r) can be adjusted while repeating steps (2) to (5). This allows for the study of the relationship between the AMM signal and error variation resulting from changes in well spacing.

Furthermore, by adjusting the direction (represented as θ) of the straight conductor and the probe while repeating steps (2) to (5), researchers can simulate different wellbore attitudes. This facilitates the investigation of the relationship between the AMM signal and error variation caused by changes in wellbore direction.

Overall, by using these methods to simulate different scenarios, the relationship between the AMM signal and error variation can be better understood, leading to more accurate and reliable measurements in the field.

4. Result Analysis

4.1. Analysis of distance measurement results.

Based on the experimental setup shown in Figure 3 a simulated experimental platform was created that maintained the positions of the experimental system and the accident well casing. To simulate the control of the relative position between two wells, the hydraulic control system was used to adjust the probe's position. The main objective of this process was to validate the accuracy of the relief well inversion theory. Researchers were able to conduct an inversion of the relative distance between the two wells by monitoring the changes in the measurement signal received by the probe. The magnetic field strength and its corresponding actual distance were determined and rigorously verified several times. Finally, the calibration of the relationship between magnetic field strength

and distance was achieved.

During the experiment, other parameters were kept constant while the r value was adjusted, and the magnetic field amplitude was measured using a probe for distances of 0.2m, 0.3m, and 0.4m. The measured magnetic field signal was then transmitted to the processing system, and an active magnetic measurement algorithm was employed to store and process the signal. Ultimately, the processed results were compared to both the theoretically calculated magnetic field strength and the orientations obtained from APS. Table 1 presents the magnetic field intensity data corresponding to different distances.

Table 1. Magnetic field data at different distances

r	Approximate	Ture	Measurd	Deviation
0.2(m)	66.56(nT)	55.27(nT)	63.85(nT)	16%
0.3(m)	43.35(nT)	33.31(nT)	35.93(nT)	8%
0.4(m)	31.51(nT)	22.63(nT)	23.65(nT)	4%

Based on the information presented in Table 1, it is evident that the magnetic field amplitude detected by the probe decreases as the distance between the accident well and the probe increases. This confirms the corresponding relationship between magnetic field strength and actual distance. Furthermore, as the distance between the probe and the accident well increases, the magnetic field strength drops sharply at a cubic rate.

The deviation between the approximate and actual magnetic field strengths decreases gradually as the distance between the probe and the well increases. The rate of increment in deviation slows down as the distance increases. At a distance of 0.4 meters (r=0.4 m), the deviation in the magnetic field strength is approximately 4%.

4.2. Analysis of azimuth measurement results

The accuracy of this concept was tested and verified using the distance and azimuth algorithm, and a simulated experimental platform was created based on the experimental set-up elaborated in Figure 3. By leveraging spatial geometry, it is possible to precisely determine the azimuth between two wells, given the known relative distance between them.

During the course of the experiment, the high-side was set as the reference point, while all other parameters were held constant. The relative position between the two wells was varied, with measurements taken every 60°, starting from 0° and covering between 0-300°. Additionally, the angle of inclination of the two simulated wells was altered to 60°, 75°, and 90°, respectively, and measurements were taken multiple times.

The directional data processed by algorithms can be found in Table 2. This shows a comparison of theoretical and actual high-side orientation errors under different well deviation conditions. It is worth noting that under the specific condition in which two wells are parallel to one another, the influence of well deviation on the high-side orientation results can be safely ignored.

Table 2. Magnetic field data at different distance

Well inclination (°)	True high side (°)	Measured high side (°)	Deviation (°)
60	0	7.524	7.524
	60	58.8915	-1.1085
	120	117.9975	-2.0025
	180	187.1815	7.1815
	240	241.8077	1.8077
	300	309.2463	9.2463
75	0	7.5023	7.5023
	60	58.452	-1.548
	120	117.4192	-2.5808
	180	187.5126	7.5126
	240	243.1918	3.1918
	300	309.9885	9.9885
90	0	7.7636	7.7636
	60	58.5286	-1.4714
	120	116.8625	-3.1375
	180	188.1316	8.1316
	240	243.1274	3.1274
	300	310.0829	10.0829

4.3. Magnetic interference measurement experiment

During the third and fourth stages of the relief well construction project, which involves the accompanying tracking and well-eye connection processes, there is a strong magnetic field interference near the casing. This interference can adversely affect the reliability of active magnetic measurements and result in decreased measurement accuracy. Therefore, calibration experiments need to be conducted on the ground before conducting on-site tests.

With reference to the experimental device in Figure 3, an experimental platform was established by selecting different points in two directions at azimuth angles of 176.4° and 92.6°, respectively. In Figure 5, O and P represent the locations of the casing and probe, respectively, and R represents the distance between them. During the experiment, all other parameters were held constant, while the distance R was

varied. Magnetic field signals were recorded using the probe under different conditions and transmitted to the processing system for calculating the relative position between two wells. The calculated results were then compared to the azimuth values measured by APS.

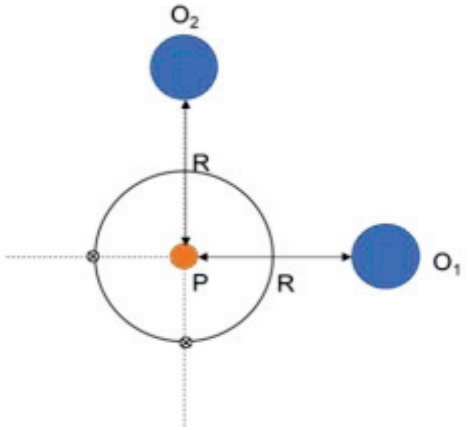

Figure 5. Experimental top view

The well inclination, self-orientation, magnetic inclination, and magnetic intensity were compared using static data verification in Table 1 for both directions. The results indicate that the well inclination, self-orientation, magnetic inclination, and magnetic intensity gradually stabilize when the distance between the casing of the incident well and the probe exceeds 1m. This suggests that magnetic interference decreases with distance, which is a positive finding for the accuracy of magnetic measurements in wellbore positioning.

Table 1. Static Data Verification Table

Distance (m)	Azimuth(°)	Well inclination (°)	Self-azimuth (°)	Magnetic inclination angle(°)	Magnetic total intensity (nT)
0.5	176.4	0.54	240.18	58.57	44818.99
1		0.55	241.87	59.42	49710.66
1.5		0.54	241.94	60.04	51305.23
2		0.54	241.12	60.32	51896.24
2.5		0.54	241.22	60.45	52155.66
3		0.56	240.63	60.53	52288.93
0.5	92.6	0.55	246.31	55.64	46116.74
1		0.55	242.13	58.87	49995.68
1.5		0.55	241.81	59.89	51431.65
2		0.55	241.13	60.30	52077.28
2.5		0.54	241.29	60.49	52269.40
3		0.53	240.61	60.58	52406.42

To obtain the azimuth deviation comparison chart, the relative azimuth measured by the probe is compared with the APS azimuth. The chart shows that as the distance between the wells increases, the deviation of the measurement azimuth gradually diminishes. Once the distance between the two wells surpasses 1m, the deviation of the measured azimuth is within 5°, implying an increased level of accuracy. Additionally, with a deviation of less than 92.6° at the equal distance azimuth of 176.4°, the measurement is considered more precise.

5. Conclusion

This paper describes a physical simulation experiment that assesses the performance of a linear electrode-based relief well positioning and detection system. The system is designed to locate relief wells near accident well casings using a straight wire and probe. The experiment simulates the distance measurement between the probe and the straight wire by adjusting the distance between them to simulate the relative position of the two wells. The results show that as the distance between the probe and the accident well increases, the magnetic field strength sharply decreases at a cubic speed, and the deviation between the estimated and true magnetic field strength gradually increases at a slower rate.

The direction measurement of the system is validated by simulating the relative orientation between the two wells and using the distance direction algorithm. The experiment concludes that the high side direction algorithm has an average error within 5°, which is suitable for practical engineering applications. Additionally, under the condition of two parallel wells, the effect of well deviation on the high side direction can be ignored.

To verify the interference of strong magnetic fields near the casing, a ground magnetic field interference calibration experiment is conducted. The results show that when the distance between the accident well casing and the probe exceeds 1m, the well deviation angle, self-orientation, magnetic inclination angle, and total magnetic field gradually stabilize, indicating that magnetic interference weakens as the distance increases.

Overall, the experimental results demonstrate that the linear electrode-based relief well positioning and detection

system has excellent performance, displaying high accuracy and small errors, making it suitable for practical engineering applications.

References

[1] Aadnoy B S, Rogaland U. Relief Well Breakthrough at Problem Well 2/4-14 in the North Sea. SPE 20915, 1990.

[2] Paula, D. (2018). Relief-well drilling enhanced to pump more kill mud. J. Oil & Gas Journal, 116(9): 1356-1359.

[3] Maehs, J, Macafee, D, Renne, S. (2008). Successful relief well drilling utilizing gyroscopic MWD (GMWD) for reentry into an existing cased hole. SPE R., 116274.

[4] Jones, D. L, Hoehn, G. L, Kuckes, A. F. (1987). Improved magnetic model for determination of range and direction to a blowout well. SPE R., 14388.

[5] Kuckes, A. F. Single-wire guidance system for drilling boreholes. (1996). U. S. Patent 5, 515, 931.

[6] Vanessa, F. Penny, A. David, T. Relief well planning. (2008). SPE 168092, 2014.

[7] Pratt, C. K, Hartman, R. A. A Magnetostatic well tracking technique for drilling of horizontal parallel wells. (1994). SPE 28319, 1994.

[8] Kuckes, A. F. An electromagnetic survey method for directionally drilling a relief well into a blow out oil or gas well. (1983). SPE 10946.

[9] Edvardsen, E., Nyrnes, M. G. Johnsen, T. L. Hansen (retired), I.. Aarnes. How To Manage Geomagnetic-Field Disturbances in the Northern Auroral Zone to Improve the Accuracy of Magnetic Measurement-While-Drilling Directional Surveys.America: Society of petroleum engineers. (2019, June)

[10] Jean Paul Lips, Georgy Rassadkin, and Jamie Dorey..Connecting Wells in Environmentally Sensitive Areas Using Magnetic Ranging-While-Drilling Technology for Enhanced Hydrocarbon Recovery. Society of Petroleum Engineers. (2020，July 20)

[11] Rassadkin, G., Ridgway, D., Moss, C.J. Using Simultaneous Gyro Measurements to Determine Orientation of Magnetic Ranging Instruments in a Vertical Environment. Society of Petroleum Engineers. SPE 190979. (2018, August 24).

[12] Vandal B, Grills T, Wilson G. A comprehensive comparison between the magnetic guidance tool and the rotating magnet ranging service. Canada: Petroleum society of Canada 2004: 1-9.

[13] Jean Paul Lips, Georgy Rassadkin, and Jamie Dorey..Connecting Wells in Environmentally Sensitive Areas Using Magnetic Ranging-While-Drilling Technology for Enhanced Hydrocarbon Recovery. Society of Petroleum Engineers. (2020，July 20)